SIAM J. Applied Dynamical Systems
Vol. 13, No. 1, pp. 276–305

Optimal Chaotic Desynchronization for Neural Populations*

Dan Wilson† and Jeff Moehlis†

Abstract. A procedure is developed for finding an energy-optimal stimulus which gives a positive Lyapunov exponent, and hence desynchronization, for a neural population. The procedure is illustrated for three different neural models. Not only does it achieve desynchronization for each model, but it also does so using less energy than recently proposed methods, suggesting a powerful alternative to pulsatile stimuli for deep brain stimulation. Furthermore, we calculate error bounds on the optimal stimulus which will guarantee a minimum Lyapunov exponent. Also, a related control strategy is developed for desynchronizing neurons based on the population's phase distribution.

Key words. optimal control, chaotic desynchronization, Parkinson's disease, deep brain stimulation

AMS subject classifications. 92C20, 65K10, 34H10

DOI. 10.1137/120901702

1. Introduction.

Pathological synchronization among spiking neurons in the basal ganglia–cortical loop within the brain is thought to be one factor contributing to the tremors exhibited by patients with Parkinson's disease [9]. Deep brain stimulation (DBS), a well-established technique for mitigating these tremors, has been hypothesized to desynchronize these neurons through the injection of a high-frequency, pulsatile input into an appropriate region of the brain [26], [38], [41]. Typically, DBS is implemented with a permanent, high-frequency, pulsatile signal which is administered in an open-loop fashion. This has motivated researchers to search for alternative stimuli that consume less energy in order to prolong stimulator battery life and to mitigate side effects of DBS such as aggregate tissue damage. Control methods that employ feedback control are of particular interest because they can be used only when needed. For example, in [37], double-pulse stimulation was shown to desynchronize a population of noisy phase oscillators and prevent resynchronization. Nonlinear, time-delayed feedback was used in [21] to experimentally desynchronize a system of electro-chemical oscillators. In [3], a minimum time desynchronizing control based on phase resetting for a coupled neural network was established using a Hamilton–Jacobi–Bellman approach, which was later extended by [24] to desynchronize neurons using an energy-optimal criterion. In [4], an energy-optimal, charge-balanced stimulus was used to control neural spike timing. More recently, [36] developed a model to control neural networks using a light-sensitive protein instead of electrical stimuli.

In this work, we present a procedure for finding an energy-optimal DBS stimulus which exponentially desynchronizes a population of coupled neurons. An advantage of this approach is that it requires only knowledge of a neuron's phase response curve (PRC), which is experimentally measurable by perturbing an oscillatory neuron at different phases and determining

*Received by the editors December 7, 2012; accepted for publication (in revised form) by T. Sauer September 6, 2013; published electronically March 4, 2014.
http://www.siam.org/journals/siads/13-1/90170.html
†Mechanical Engineering Department, University of California at Santa Barbara, Santa Barbara, CA 93106 (dan.d.wilson8@gmail.com, moehlis@engineering.ucsb.edu).

the change in spike timing [25]. Unlike the methods in [3] and [24], our approach does not need the full model for the dynamics, and unlike [10] and [4], it requires only a single input. Methods presented in [33], [29], [40], [31], [22], and [30] use delayed-feedback stimulation to counter the effects of mean-field coupling on an ensemble of heterogeneous oscillators, and the method presented in this work notably differs from these methods because it is applicable to networks without mean-field coupling and does not require simultaneous stimulation and measurement. We compare this method to other recently proposed methods, to show not only its desynchronizing capabilities for many types of neural models, but also its ability to act with comparatively small control inputs. Furthermore, we compute error bounds on the optimal stimulus that will guarantee a resulting signal with the properties required to desynchronize a network of neurons, and propose a control strategy for desynchronizing a population based on its phase distribution.

The organization of the paper is as follows. In section 2, we derive an expression for the Lyapunov exponent for two neurons with similar initial phases and use the result to develop a control method. Section 3 uses the optimal stimulus calculated in section 2 to develop sufficient conditions for obtaining a stimulus with a predetermined guarantee on its Lyapunov exponent. In section 4 we develop a control methodology based on a population's phase distribution. Section 5 examines the control methodology applied to three neural models in order to make comparisons with previous work. Section 6 gives concluding comments.

2. Derivation of the Lyapunov exponent and optimal control. We present a procedure for finding an energy-optimal DBS stimulus which exponentially desynchronizes a population of neurons. An advantage of this approach is that it requires only knowledge of a neuron's PRC, which is experimentally measurable by perturbing an oscillatory neuron at different phases and determining the change in spike timing [25]. The PRC can also be calculated numerically if all equations and parameters in the neural model are known; see e.g., [2]. Through phase reduction, as illustrated, for example, in [2], we can obtain a reduced model for a single neuron of the form

$$\frac{d\theta}{dt} = \omega + Z(\theta)u(t), \tag{1}$$

where θ is the phase of the neuron and is 2π-periodic on $[0, 2\pi)$ and, by convention, $\theta = 0$ corresponds to the spiking of the neuron. Here, ω gives the neuron's baseline dynamics, which are determined from its natural period T as $\omega = 2\pi/T$; $Z(\theta)$ is the PRC; and $u(t) = I(t)/C$, with $I(t)$ being the control input and $C = 1\mu\text{F/cm}^2$ being the constant neural membrane capacitance.

Lyapunov exponents are commonly used to describe the rate at which nearby trajectories diverge, and they have proven useful in other problems, for example, by serving as biomarkers for seizure prediction and control [16], [15], [28]. We now derive an expression for the Lyapunov exponent for (1) by considering two identical neurons subject to a common stimulus:

$$\frac{d\theta_i}{dt} = \omega + Z(\theta_i)u(t), \quad i = 1, 2. \tag{2}$$

Here we assume that the neurons are nearly in-phase, so that $\theta_1 \approx \theta_2$. Letting $\phi \equiv |\theta_2 - \theta_1|$,

we obtain

$$\frac{d\phi}{dt} = Z'(\theta)u(t)\phi + \mathcal{O}(\phi^2). \tag{3}$$

Since we have linearized the equation, we assume that solutions are of the form $\phi \sim e^{\Lambda t}$, which yields the finite time Lyapunov exponent (cf. [1])

$$\Lambda(\tau) = \frac{\log(\phi(\tau))}{\tau} = \frac{\int_a^{a+\tau} Z'(\theta(s))u(s)ds}{\tau}. \tag{4}$$

We now consider a population of neurons, each described by an equation of the form (1). Suppose that for some time t_1, for all stimuli $u(t)$ that advance θ from $\theta(0) = 0$ to $\theta(t_1) = \omega t_1$ (that is, stimuli that do not create any net change of phase), we want to find the stimulus that minimizes the cost function $G[u(t)] = \int_0^{t_1}[u(t)^2 - \beta Z'(\theta(t))u(t)]dt$. Here, $\int_0^{t_1}[u(t)^2]dt$ corresponds to the power associated with the stimulus, and $\beta > 0$ is a scaling parameter that determines the relative importance of minimizing the energy versus maximizing the Lyapunov exponent, $\Lambda(t_1)$. We apply calculus of variations to minimize [7]

$$\mathcal{C}[u(t)] = \int_0^{t_1} \left\{ u(t)^2 - \beta Z'(\theta)u(t) + \lambda \left(\frac{d\theta}{dt} - \omega - Z(\theta)u(t) \right) \right\} dt, \tag{5}$$

where the Lagrange multiplier λ forces the neural dynamics to obey (1). The resulting Euler–Lagrange equations are

$$u(t) = [\beta Z'(\theta) + \lambda Z(\theta)]/2, \tag{6}$$

$$\dot{\theta} = Z(\theta)\left[\beta Z'(\theta) + \lambda Z(\theta)\right]/2 + \omega, \tag{7}$$

$$\dot{\lambda} = -\left[\beta Z'(\theta) + \lambda Z(\theta)\right]\left[\beta Z''(\theta) + \lambda Z'(\theta)\right]/2, \tag{8}$$

where $' = d/d\theta$. To find the optimal control, $u(t)$, (7) and (8) must be solved subject to the boundary conditions $\theta(0) = 0$, $\theta(t_1) = \omega t_1$. This can be done by numerically finding the initial condition $\lambda(0) \equiv \lambda_0$ that satisfies the boundary conditions, for example, by using a shooting method. We note that the above conditions are only necessary and not sufficient for global optimality. However, the phase reduction (1) requires inputs of small amplitude so that solutions remain close to the periodic orbit. Since $u(t)$ is directly proportional to λ in (6), we can limit our search to include solutions obtained with reasonably small values of $\lambda(0)$ in order to find a feasible solution.

While the previous procedure will produce an energy-optimal stimulus, it will not necessarily be charge-balanced (CB). The importance of CB stimuli in DBS has been known for many years. Over time, non–charge-balanced (NCB) stimuli can create an accumulation of charge and cause harmful Faradaic reactions that may damage surrounding neural tissue or the DBS electrode [23]. If we consider the total charge q imparted to a neuron to be the integral of the current, then $\dot{q}(t) = Cu(t)$, and we can derive an optimal CB stimulus by optimizing the same cost function as in the NCB case, $G[u(t)]$, subject to the additional constraints $q(0) = 0$ and $q(t_1) = 0$, the latter ensuring that the stimulus will be charge neutral at t_1. We again

apply calculus of variations [7] to minimize $\mathcal{C}[\mathbf{\Phi}(t), \dot{\mathbf{\Phi}}(t), u(t)] = \int_0^{t_1} \mathcal{M}[u(t)]dt$, where

$$\mathcal{M}[u(t)] = u(t)^2 - \beta Z'(\theta)u(t) + \begin{bmatrix}\lambda_1(t) & \lambda_2(t)\end{bmatrix} \begin{bmatrix}\frac{d\theta}{dt} - \omega - Z(\theta)u(t) \\ \frac{dq}{dt} - u(t)\end{bmatrix} \tag{9}$$

and $\mathbf{\Phi}(t) = [\theta(t), q(t), \lambda_1(t), \lambda_2(t)]^T$. The Lagrange multipliers λ_1 and λ_2 force the dynamics to satisfy the evolution equations for θ and q given above. The associated Euler–Lagrange equations are

$$\frac{\partial \mathcal{M}}{du} = \frac{\partial}{\partial t}\left(\frac{\partial \mathcal{M}}{\partial \dot{u}}\right), \qquad \frac{\partial \mathcal{M}}{d\mathbf{\Phi}} = \frac{\partial}{\partial t}\left(\frac{\partial \mathcal{M}}{\partial \dot{\mathbf{\Phi}}}\right). \tag{10}$$

With the above boundary conditions, this is a two-point boundary value problem for $u(t)$ which is solved using a double bisection algorithm described in [4]. As with the NCB formulation, (10) is only necessary and not sufficient for global optimality, but we can limit our search for $\lambda_1(0)$ and $\lambda_2(0)$ so that the resulting solutions yield optimal stimuli that are small enough that the phase reduction (1) is still valid.

3. Guaranteed Lyapunov exponents. In an experimental setting, errors in measuring the PRC will induce errors in the calculated optimal stimulus. An important question to ask is whether or not these errors will stifle the desynchronizing efforts of the electrical signal, and how large these errors need to be before they completely degrade its desynchronizing capabilities. To answer these questions, we consider an NCB optimal stimulus, $I_{opt}(t)$, found using methods from section 2. Consider another stimulus, $I_c(t)$, that is different from $I_{opt}(t)$. We define the error signal as $I_e(t) = I_c(t) - I_{opt}(t)$ and the infinity norm of $I_e(t)$ as

$$||I_e(t)||_\infty = \sup_{0 \le t \le t_1} |I_e(t)|, \tag{11}$$

where t_1 is the duration of the optimal signal. As we will demonstrate in section 5, a signal with a larger Lyapunov exponent will desynchronize two neurons with similar initial phase more quickly. For this reason, we use the Lyapunov exponent from (4) as a measure of the desynchronizing capabilities of a signal. In order to identify a bound on $||I_e(t)||_\infty$ which can guarantee desynchronization, we must find the worst possible Lyapunov exponent for any signal with $||I_e(t)||_\infty \le E$, where E is a constant. To do so, we define the cost function $\mathcal{L}[I_e(t)] = \int_0^{t_1} [I_{opt}(t) + I_e(t)]Z'(\theta(t))dt$ subject to (1), $\dot{\theta} = \omega + Z(\theta)[I_{opt}(t) + I_e(t)]$, with the additional constraint $-E \le I_e(t) \le E$ for all $t \in [0, t_1]$. Here, $\mathcal{L}[I_e(t)]$ corresponds to the Lyapunov exponent for a stimulus $I_c(t)$. The inequality constraint ensures that $||I_e(t)||_\infty \le E$. Using Pontryagin's minimum principle [20], a necessary condition for the control that minimizes $\mathcal{L}[I_e(t)]$ is that the control minimize the Hamiltonian

$$\mathcal{H}(\theta(t), I_e(t), p_1(t)) = [I_{opt}(t) + I_e(t)]Z'(\theta(t)) + \omega p_1(t) + [I_{opt}(t) + I_e(t)]p_1(t)Z(\theta(t)) \tag{12}$$

and be given by $I_e(t) = -E\text{sign}(Z'(\theta) + p_1(Z(\theta))$, where $' = d/d\theta$ and p_1 is a Lagrange multiplier. Furthermore,

$$\dot{\theta} = \omega + Z(\theta)[I_{opt}(t) + I_e(t)], \tag{13}$$

$$\dot{p_1} = -[I_{opt}(t) + I_e(t)]Z''(\theta) - p_1 Z'(\theta)[I_{opt}(t) + I_e(t)], \tag{14}$$

with the boundary condition $\theta(0) = 0$. From the problem formulation, we have only one boundary condition, and in order to find the global minimum of $\mathcal{L}[I_e(t)]$, we must simulate (13) and (14) for all plausible values for $p_1(0)$ to determine the minimum (worst case) Lyapunov exponent of the associated signals. Using this approach, we can find boundaries on a stimulus that are sufficient, but not necessary, to yield a given Lyapunov exponent.

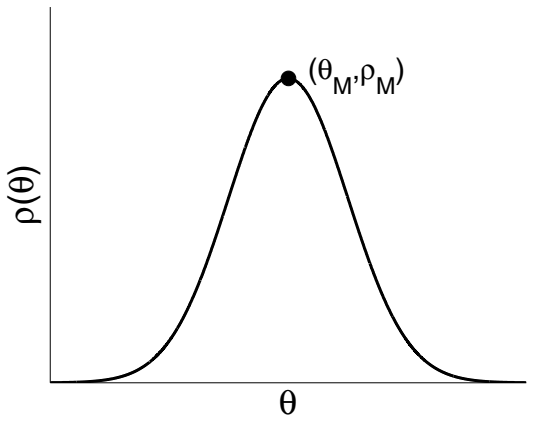

Figure 1. *The maximum value, ρ_M, for a large distribution of neurons.*

4. Optimal control of the phase distribution. The methods from section 2 are optimal for desynchronizing two neurons with close initial phase. However, brain regions can contain on the order of billions of neurons [27]. For large populations of neurons, rather than examining individual neurons, which can be too large to simulate in silico, it is appropriate to monitor the probability density of neurons with phase θ at a given time, $\rho(\theta, t)$. For an uncoupled population that obeys (1), the probability density evolves according to the advection equation, as described in [38]:

$$\frac{\partial \rho(\theta,t)}{\partial t} = -\frac{\partial}{\partial \theta}\left[\{\omega + Z(\theta)u(t)\}\,\rho(\theta,t)\right] = -\rho\frac{\partial \nu}{\partial \theta} - \nu\frac{\partial \rho}{\partial \theta}, \tag{15}$$

where $\nu(\theta, t) = \omega + Z(\theta)u(t)$. In section 5, we show that the CB and NCB optimal signals obtained using methods from section 2 can effectively desynchronize a network of 100 coupled neurons for many different neural models. Therefore, it is no surprise that the same signal is effective at desynchronizing a population evolving according to (15) (not shown).

However, we wish to approach this problem from a neural population perspective, to see if we can find an effective control strategy to desynchronize large neural populations. Suppose that we are interested in the evolution of the maximum of the distribution, ρ_M, at $\theta \equiv \theta_M$; see Figure 1. Noting that the total time derivative of the distribution is $\frac{d\rho}{dt} = \frac{\partial \rho}{\partial t} + \frac{\partial \rho}{\partial \theta}\frac{d\theta}{dt}$, and that $\frac{\partial \rho}{\partial \theta} = 0$ at the local maximum, we find

$$\frac{d\rho_M}{dt} = -\rho_M \frac{\partial \nu}{\partial \theta}(\theta_M, t) = -Z'(\theta_M)u(t)\rho_M. \tag{16}$$

Note the similarity of (16) to (3). From the two-neuron optimal control formulation, $Z'(\theta)u(t) > 0$ corresponds to increasing the phase difference, whereas here it corresponds to a decreasing value of ρ_M. In order to find an equation for the evolution of θ_M, we again make use of the relation $\frac{\partial \rho}{\partial \theta}|_{\theta_M} = 0$. Taking the total time derivative yields

$$\begin{aligned} 0 &= \frac{\partial}{\partial \theta}\frac{d\rho}{dt} \\ &= \frac{\partial}{\partial \theta}\left[\rho_\theta \frac{d\theta_M}{dt} + \rho_t\right] \\ &= \frac{\partial}{\partial \theta}\left[\rho_\theta \frac{d\theta_M}{dt} - \nu_\theta \rho - \rho_\theta \nu\right], \end{aligned}$$

$$\rho_{\theta\theta}\frac{d\theta_M}{dt} = \nu_{\theta\theta}\rho + 2\nu_\theta \rho_\theta + \rho_{\theta\theta}\nu. \tag{17}$$

All expressions in the above equation are evaluated at ρ_M and θ_M; thus $\rho_\theta = 0$. Also, since ρ_M is a local maximum, $\rho_{\theta\theta} < 0$, and (17) becomes

$$\frac{d\theta_M}{dt} = \omega + Z(\theta)u(t) + \frac{\rho_M}{\rho_{\theta\theta}}Z''(\theta)u(t). \tag{18}$$

Equations (16) and (18) are special cases of the equations derived in [32]. In order to effectively use (18), we must find some function $\kappa(\theta_M, \rho_M) \approx \rho_{\theta\theta}$. One such κ, which works well in practice, can be obtained by starting with a Gaussian distribution and assuming that the distribution remains Gaussian for all time. We note that while the phase reduction is valid for $\theta \in [0, 2\pi)$, a Gaussian distribution is defined for all θ. However, because we are considering synchronized systems with a small variance, the values of the Gaussian distribution that we are ignoring are insignificant. Using this strategy, one can easily show that $\kappa(\rho_M) = -2\pi\rho_M^3$.

Equation (16) is separable, and we can solve explicitly to determine the change in the value of ρ over some time interval of length T:

$$\begin{aligned} \int_a^{a+T} \frac{1}{\rho_M} d\rho_M &= -\int_a^{a+T} Z'(\theta_M)u(t)dt \\ \implies \log\left(\frac{\rho_M(a+T)}{\rho_M(a)}\right) &= -\int_a^{a+T} Z'(\theta_M)u(t)dt. \end{aligned} \tag{19}$$

If we want to minimize ρ_M while taking into account the energy expended, we can use calculus of variations [7] to minimize $\mathcal{C}[\mathbf{\Phi}(t), \dot{\mathbf{\Phi}}(t), u(t)] = \int_0^{t_1} \mathcal{G}[u(t)]dt$, where

$$\mathcal{G}[u(t)] = u(t)^2 - \beta Z'(\theta)u(t) + \begin{bmatrix}\lambda_1(t) & \lambda_2(t)\end{bmatrix}\begin{bmatrix}\frac{d\theta}{dt} - \omega - Z(\theta)u(t) - \frac{\rho_M}{\kappa(\theta_M,\rho_M)}Z''(\theta)u(t) \\ \frac{d\rho_M}{dt} + \rho_M Z'(\theta)u(t)\end{bmatrix} \tag{20}$$

and $\mathbf{\Phi}(t) = [\theta_M(t), \rho_M(t), \lambda_1(t), \lambda_2(t)]^T$. Lagrange multipliers λ_1 and λ_2 force the dynamics to satisfy (16) and (18). Note the similarity of (20) to the NCB cost function (5). When $\kappa(\theta_M, \rho_M) \gg \rho_M Z''(\theta)u(t)$ (as might be the case for a highly synchronized network), the

function that minimizes (20) is approximately the same function that minimizes (5). Taking $\kappa(\rho_M) = -2\pi\rho_M^3$ as previously mentioned, the associated Euler–Lagrange equations are

$$u(t) = \left[\beta Z'(\theta_M) + \lambda_1\left(Z(\theta_M) - \frac{1}{2\pi\rho_M^2}Z''(\theta_M)\right) - \lambda_2\rho_M Z(\theta_M)\right] \Big/ 2, \tag{21}$$

$$\dot{\rho_M} = -\rho_M Z'(\theta_M)u(t), \tag{22}$$

$$\dot{\theta_M} = \omega + Z(\theta_M)u(t) - \frac{1}{2\pi\rho_M^2}Z''(\theta_M)u(t), \tag{23}$$

$$\dot{\lambda_1} = \lambda_1 u(t)\left[\frac{1}{2\pi\rho_M^2}Z'''(\theta_M) - Z'(\theta_M)\right] + Z''(\theta_M)u(t)\left[\rho_M\lambda_2 - \beta\right], \tag{24}$$

$$\dot{\lambda_2} = u(t)\left[-\frac{\lambda_1 Z''(\theta_M)}{\pi\rho_M^3} + \lambda_2 Z'(\theta_m)\right]. \tag{25}$$

Unlike the problem for finding the maximum Lyapunov exponent, the distribution minimization problem depends on the initial height of the distribution, $\rho_M(0)$. We will take $\theta_M(0) = 0$, which leaves two initial conditions to be determined later.

5. Results and discussion.

5.1. Maximizing Lyapunov exponents for the thalamus model. Because pathological neural synchronization in the thalamus is thought to play an important role in Parkinson's disease [9], we consider a three-dimensional model to describe thalamic neural activity [34]:

$$\begin{aligned}\dot{V_i} = \Bigg(&- I_L(V_i) - I_{Na}(V_i, h_i) - I_K(V_i, h_i) - I_T(V_i, r_i) \\ &+ I_{SM} + \frac{1}{N}\sum_{i=1}^{N}\alpha_{ij}(V_j - V_i) + u(t) + \eta_i(t)\Bigg) \Big/ C, \\ \dot{h_i} &= (h_\infty(V_i) - h_i)/\tau_h(V_i), \\ \dot{r_i} &= (r_\infty(V_i) - h_i)/\tau_r(V_i), \quad i = 1, \ldots, N.\end{aligned} \tag{26}$$

We have augmented the voltage equation by additively including electrotonic coupling [18], DBS input, and Gaussian white noise. Here, N is the total number of neurons; V_i, h_i, and r_i are membrane voltage and gating variables for neuron i; α_{ij} characterizes the coupling strength between electrotonically coupled neurons i and j, with $\alpha_{ij} = \alpha_{ji}$ and $\alpha_{ii} = 0$ for all i; $\eta_i(t) = \sqrt{2D}\mathcal{N}(0,1)$ is the independent and identically distributed (i.i.d.) noise associated with each neuron, assumed to be zero-mean Gaussian white noise with variance $2D$; and $u(t) = I(t)/C$ represents a common control input. In this equation I_{SM} represents the baseline current, which we take to be $5\mu\text{A/cm}^2$. For a full explanation of the functions $I_L, I_{Na}, I_K, I_t, h_\infty, \tau_h, r_\infty$, and τ_r, we refer the reader to [34].

The baseline current causes the neuron to fire with period $T = 8.395$ms. To obtain the optimal control, we take $t_1 = 7.35$ms (corresponding to $\theta = 5.5$ on the limit cycle) and $\beta = 40$. Note that t_1 sets the duration of the stimulus and could be chosen differently, provided that it is sufficiently smaller than T, and β has been chosen so that a positive Lyapunov exponent

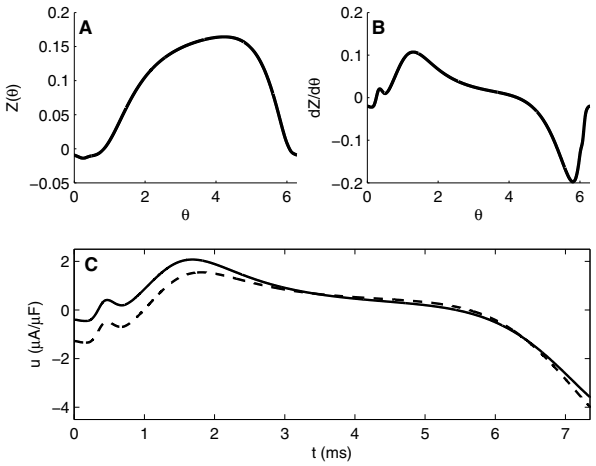

Figure 2. *Numerically computed PRC* (A) *and its derivative* (B) *for the thalamus model* (26). (C) *The CB and NCB optimal stimuli are shown as dashed and solid lines, respectively.*

is favored but also so that the magnitude of the control input is small enough so that the phase reduction from (1) is still valid. We solve (7) and (8) numerically with a fourth order Runge–Kutta solver, and the optimal control is found from (6). We do the same for the Euler–Lagrange equations from (10).

Panels (A) and (B) of Figure 2 show the PRC and its first derivative for (26), numerically obtained using the software X-Windows Phase Plane (XPP) [6]. Panel (C) of Figure 2 shows the optimal CB and NCB stimuli. Both stimuli are similar because the NCB stimulus is nearly CB. We note that the optimal stimulus is strikingly similar to $Z'(\theta)$ for $\theta \leq 5.5$ and explain this occurrence by noting that the equation for the optimal stimulus from (6) depends directly on the sum of $\beta Z'(\theta(t))$ and $\lambda(t)Z(\theta(t))$. The optimal stimulus has a relatively small magnitude, so $\theta(t) \approx \omega t$ and, numerically, we find that $\lambda(t)$ is relatively small compared to β.

In order to numerically verify that the NCB stimulus is optimal for minimizing the cost function, we analyze five other stimuli given by $u_i(t) = u_{opt}(t) + 0.5W_i(t)$, $i = 1, \ldots, 5$, where u_{opt} is the optimal NCB stimulus shown in Figure 2 and W_i is a Wiener process, added to corrupt the optimal stimulus. We note that each of these stimuli are subject to the same end point conditions described in section 2. Figure 3 shows these stimuli as well as the NCB optimal stimulus for reference. As we can see from Table 1, u_{opt} does have the best performance in terms of overall cost, but the other stimuli still yield comparable Lyapunov exponents. This prompts the question of how robust this procedure is to errors, which will be addressed later.

The Lyapunov exponents calculated using (4) for NCB and CB stimuli are 0.066 and 0.060, respectively. We find that requiring the CB constraint decreases the Lyapunov exponent and, hence, the rate of desynchronization. Figure 4 shows the phase separation of two neurons which obey (2) for the PRC found in Figure 2 subject to repeated iterations of both the NCB (panels (A) and (B)) and CB (panels (C) and (D)) stimuli. We find that the neurons exponentially desynchronize at a rate determined by their Lyapunov exponent until they are

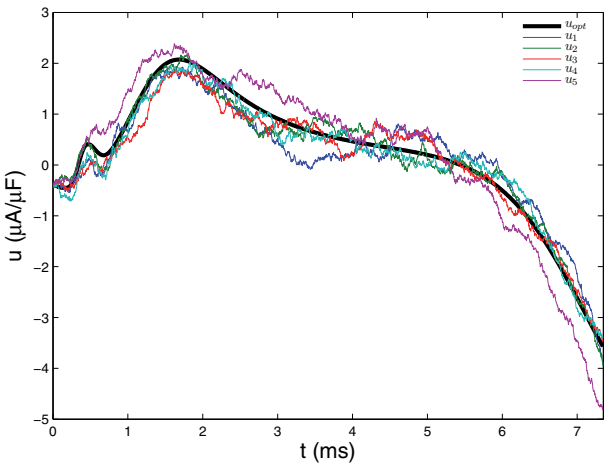

Figure 3. *The NCB optimal stimulus u_{opt} and five instances of u_{opt} that have been corrupted by noise. Indeed, out of the five stimuli, u_{opt} yields the smallest value of $\mathcal{C}[u(t)]$ from (5), but the other stimuli give values that are close to optimal.*

Table 1
Stimulus properties from Figure 3.

Stimulus	$\Lambda(T)$	Energy	$\mathcal{C}[u(t)]$
u_{opt}	0.066	11.66	-10.43
u_1	0.055	8.80	-9.68
u_2	0.062	10.7	-10.03
u_3	0.058	9.66	-9.89
u_4	0.061	10.44	-10.06
u_5	0.086	19.98	-8.95

nearly π radians out of phase. At this point, the assumption that the neurons are close in phase is no longer valid, and no further desynchronization occurs.

Results from Figure 4 apply only to neurons obeying the phase reduction (1). In order to determine the validity of the phase reduction for (26), we simulate the deterministic version of (26), i.e., with $D = 0$, using a fourth order Runge–Kutta solver. The top panel of Figure 5 shows time histories of three neurons with initial conditions that correspond to $\theta = -0.1$, 0, and $+0.1$ on the periodic orbit. The control is applied every time the reference neuron, with initial phase $\theta = 0$, fires. We find that after 70ms, the neurons no longer show any evidence of their initial synchronization.

We now apply the NCB optimal control found above to a network of $N = 100$ coupled, initially synchronized, noisy neurons, with an identical coupling strength of $\alpha_{ij} = 0.1$ and i.i.d. noise with $D = 1$, in order to test the desynchronizing effects on the full neural model. We define the mean voltage as our system observable, $\bar{V}(t) = \frac{1}{N}\sum_{i=1}^{N} V_i(t)$. The controller has two states: *active* and *inactive*. When the controller is *active*, a new stimulus is triggered when $\bar{V} > -45$mV and $\dot{\bar{V}} < 0$, with the caveat that a new stimulus cannot occur until the previous stimulus is either finished or within 0.3ms of finishing. This last condition is included to give

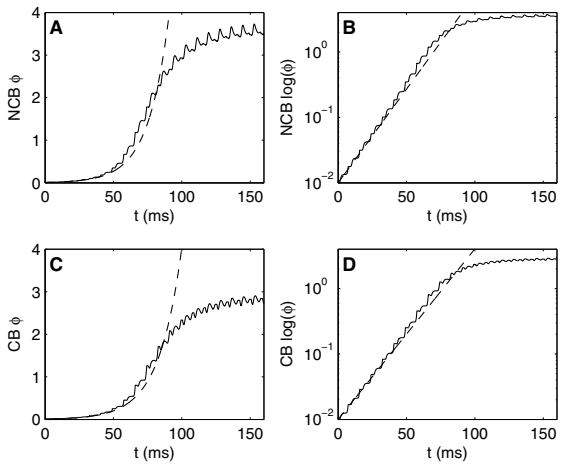

Figure 4. (A)–(B) *Phase difference between two neurons over time for the NCB optimal stimulus (giving* $\Lambda = 0.066$*) applied repeatedly to two neurons with nearly identical initial phases.* (C)–(D) *The same plots for the CB stimulus (*$\Lambda = 0.060$*). In both cases the neurons desynchronize at a rate determined by* Λ*, calculated from* (4)*, until* $\phi \approx 2$*, at which point the solution begins to asymptotically approach* $\phi \approx \pi$*, i.e., the antiphase state. Dashed lines show exponential functions based on the Lyapunov exponents.*

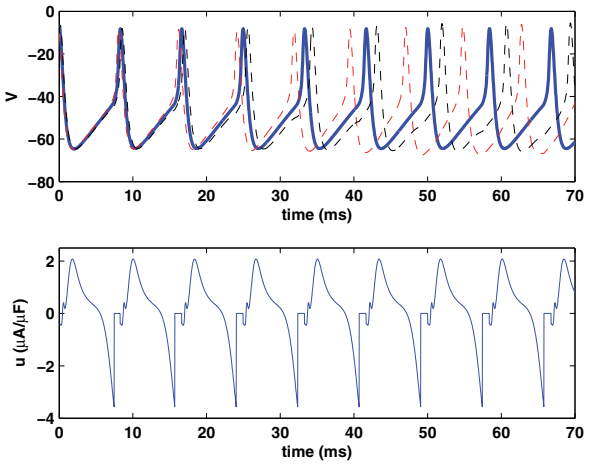

Figure 5. *Time histories of three neurons with initial conditions* $\theta = -0.1, 0,$ and $+0.1$ *on the periodic orbit. A new stimulus is applied each time the reference neuron with initial phase* $\theta = 0$ *(shown as the black curve) fires.*

the controller flexibility in when to start the next stimulus because the system is sensitive to the time when the stimulus is presented. Once $\bar{V}$ no longer spikes above -45mV, the controller changes to an *inactive* state. It changes back to the *active* state if $\bar{V}$ registers above -40mV. We use the algorithm presented in [14] to simulate the noisy system (see Figure 6). The desynchronizing effect of the stimulus can clearly be seen in the raster plot. We call this

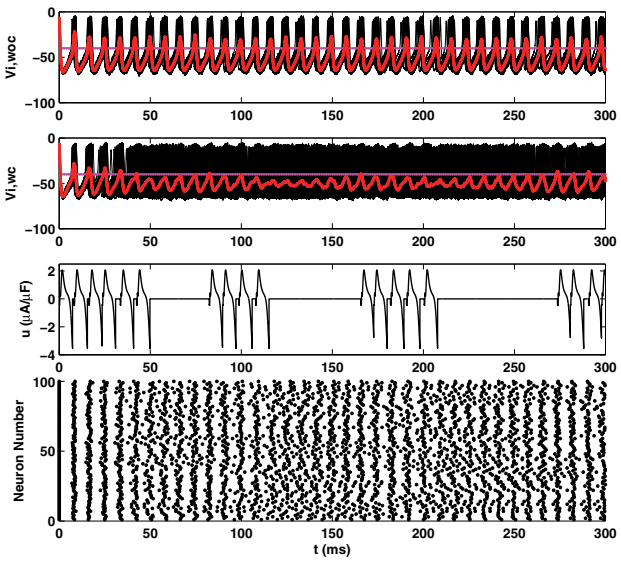

Figure 6. *Results for a population of $N = 100$ noisy, coupled neurons. The first panel shows the network in the absence of control. The second panel shows results for the same network with the event-based control applied, and the third panel shows the associated applied control. The traces give the mean voltages for the system, and the horizontal dotted line shows the control activation threshold in the top two panels. Substantial desynchronization can be seen from the raster plot at the bottom.*

event-based control because the controller is triggered only when the mean voltage crosses a certain threshold. It is worth noting that the optimal stimulus works equally well for a network of neurons that are synchronized by a common pulsatile input, which [41] suggests is the mechanism that yields synchronization. Results for such a system are qualitatively similar to the results presented in this paper.

The critical advantage of using this control strategy is that it requires knowledge only of the PRC for the system. Methods for controlling neurons that require precise knowledge of the neural model (see [24], [3]) are difficult to implement because, despite recent progress [35], it is challenging to obtain accurate full scale models of real neurons for control purposes. Methods that rely on the PRC are attractive because it is experimentally measurable. To illustrate the effectiveness of this method, we employ the following method, which we will refer to as the direct method [17], to obtain a PRC for a single neuron obeying (26). In order to obtain one data point, a short-duration pulse of current is applied to a neuron at a random phase θ, and the resulting phase change is measured by observing the change in spike time. The resulting value $Z(\theta)$ is $\frac{\Delta\theta}{Q_p/C}$, where Q_p is the total charge imparted to the neuron from the pulse and $\Delta\theta$ is the change in phase. An experimentally reasonable sampling size of 300 data points was obtained for noise levels of both $D = 1$ and 0.25, and the data was fit to a sixth order polynomial constrained to be zero at θ equals both 0 and 2π, as in [25]. The results are shown in Figure 7(A). As expected, a larger noise value yields a larger spread in the data and a less reliable PRC. The optimal stimuli obtained using the fit PRC are shown in panel (B). Finding the PRC with a D value of 0, 0.25, and 1 yields an optimal stimulus

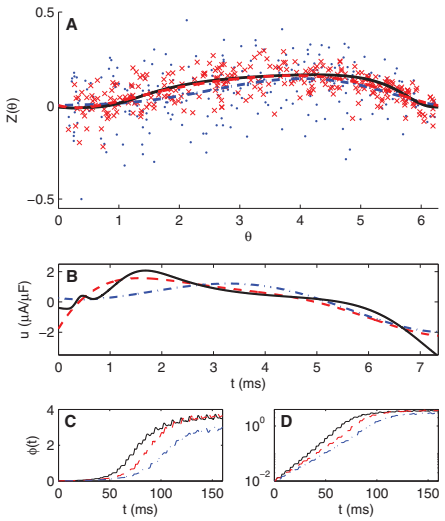

Figure 7. (A) *Obtaining the PRC from a noisy system with the direct method. Data points associated with noise level* $D = 1$ *and* 0.25 *are shown as dots and x's, respectively, with the sixth order polynomial fits given as a dashed and dot-dashed lines, respectively. Pearson correlation coefficients of the polynomial fits for* $D = 1$ *and* 0.25 *are* 0.3617 *and* 0.6638*, respectively. For comparison, the numerically computed (exact) PRC is shown as a solid line.* (B) *NCB optimal stimuli computed with experimentally determined PRC's with* $D = 1$ *and* 0.25 *are shown as dot-dashed and dashed lines, respectively. The true NCB optimal stimulus from Figure 2 is shown as a solid line for reference.* (C)–(D) *Phase differences between two neurons over time for the optimal stimulus obtained from systems with noise level* $D = 1$*,* 0.25*, and* 0 *applied repeatedly to two neurons with dynamics governed by the exact PRC and with close initial phase differences are shown as dot-dashed, dashed, and solid lines, respectively.*

with $\Lambda = 0.066$, 0.055, and 0.046, respectively. When we do not know the PRC exactly, the performance of the desynchronizing stimulus is somewhat degraded, as evidenced in panels (C) and (D), but the stimulus still performs remarkably well. We note that for a noise level of $D = 1$, the spread in the collected data for the PRC is similar to data previously collected for in vitro neurons [25].

Figure 8 shows results from a simulation using the optimal stimulus obtained from this data applied to 100 coupled neurons obeying (26) with the same noise and coupling parameters as the test shown in Figure 6. The stimulus still shows desynchronizing capabilities similar to the stimulus obtained from the true PRC.

To model more realistic neural networks, we include network heterogeneities. For comparison, our homogeneous network simulations will use $N = 100$, $\alpha_{ij} = 0.1$, and $I_b = 5$. Other simulations will consider network heterogeneities in coupling strength by drawing α_{ij} values from a normal distribution with mean $\bar{\alpha} = 0.1$ and a standard deviation $\sigma_\alpha = 0.02$; panel (A) of Figure 9 shows the specific distribution used for each simulation. Network heterogeneities in I_b are also considered by simulating a system with baseline currents drawn from a normal distribution (shown in Figure 9(B)). In each $N = 100$ neuron simulation, we use the same control logic as in the simulation with results shown in Figure 7 to determine when to apply

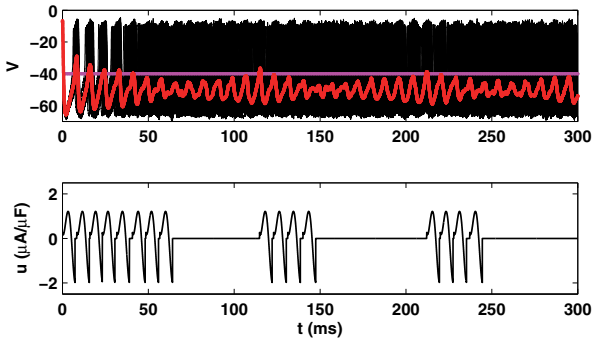

Figure 8. *Results for a population of $N = 100$ noisy, coupled neurons with optimal stimulus found using the direct method for a noisy ($D = 1$) neuron. The top panel shows the results of the network simulation, and the bottom panel shows the associated event-based control applied. The traces give the mean voltages for the system, and the horizontal dashed line in the top panel shows the control activation threshold.*

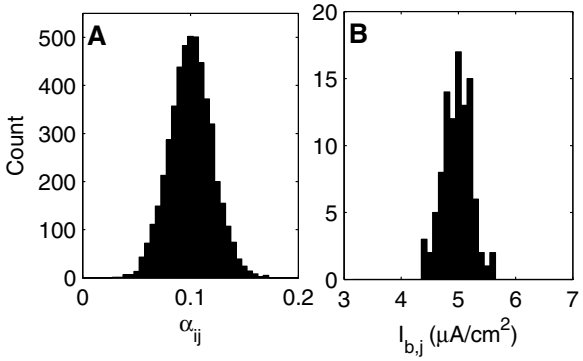

Figure 9. (A) *Normal distributions of the coupling strengths with $\alpha_{ij} \in \mathcal{N}(0.1, 0.02)$.* (B) *Normal distributions of the baseline currents with $I_{b,j} \in \mathcal{N}(5, 0.25)$.*

each new stimulus. Again, we use the algorithm presented in [14] to simulate the noisy system.

Results of each simulation are shown in Figure 10. Each row in the figure shows a network simulation (left) and the associated applied control (right). From top to bottom, the networks shown have homogeneous coupling strength and baseline current, coupling strengths drawn from a random distribution but homogeneous baseline current, baseline currents drawn from a distribution but homogeneous coupling strengths, and heterogeneous baseline and coupling strengths. For homogeneous distributions, $I_b = 5\mu A/\text{cm}^2$ and $\alpha_{ij} = 0.1$. Parameters for heterogeneous simulations are drawn from a random distribution (shown in Figure 9). We find that when we include heterogeneity, the network requires fewer applications of the optimal stimulus to desynchronize. The bottom panel shows results for a network with both heterogeneous coupling and baseline currents. Overall, we find that heterogeneity in a network decreases its tendency to resynchronize, which increases the effectiveness of the optimal control.

Clearly the optimal stimulus works well for desynchronizing a neural network, even when

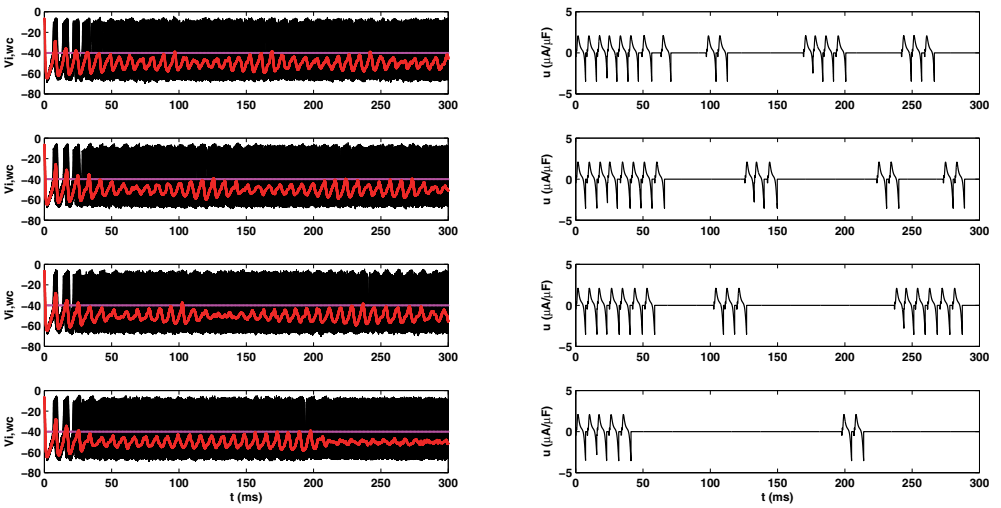

Figure 10. *Results for a population of $N = 100$ coupled neurons with i.i.d. noise strength $D = 1$. Each row in the figure shows a network simulation (left) and the associated applied control (right). From top to bottom, the networks shown have homogeneous coupling strength and baseline current, coupling strengths drawn from a random distribution but homogeneous baseline current, baseline currents drawn from a distribution but homogeneous coupling strengths, and heterogeneous baseline and coupling strengths. Once the network is sufficiently desynchronized, the controller will activate only once the voltage has crossed the threshold, shown as a horizontal line in the left set of panels.*

only an approximation to the true PRC is known. This prompts the search for error bounds on the optimal stimulus that can still guarantee desynchronization. In an ad hoc manner, using methods from section 3, we fix a particular value of E for the signal I_e and minimize (12) to find the minimal (worst case) Lyapunov exponent. We then simulate (26) with the associated signal to determine whether it can affect network desynchronization. Using this strategy with different E values, we find that, for a network of 100 neurons with homogeneous coupling $\alpha_{ij} = 0.1$ and baseline current $I_b = 5\mu\text{A/cm}^2$, we require a Lyapunov exponent of at least $\Lambda = 0.024$, corresponding to $E = 0.8$, in order to achieve sufficient desynchronization so that spikes of $\bar{V}$ remain below -40mV. Thus, $||I_e(t)||_\infty \leq 0.8$ will guarantee $\Lambda \geq 0.024$. To illustrate the utility of this measure, we choose a simple, piecewise linear signal which is contained nearly entirely in the boundary $||I_e(t)||_\infty \leq 0.8$:

$$u(t) = \begin{cases} t, & 0 \leq t \leq 2.2, \\ -4.4 - t, & 2.2 < t \leq 7.35. \end{cases} \tag{27}$$

The signal in (27) is used in a simulation of the same homogeneous network with the same control logic described previously. The results are shown in Figure 11. Numerically, we find $\Lambda = 0.0577$ for this stimulus. We note that, even though the stimulus is not entirely contained within the shaded region shown in the top panel of Figure 11 and is therefore not guaranteed to desynchronize the system, it still produces a sufficiently high Lyapunov exponent to achieve desynchronization.

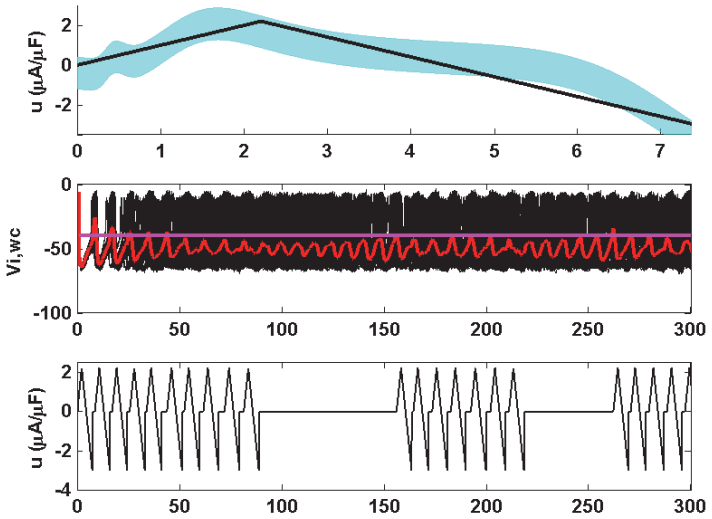

Figure 11. *Results for the population of $N = 100$ coupled neurons from Figure 4 with the simple, piecewise linear stimulus from (27). The top panel shows the stimulus as well as a shaded boundary that will ensure sufficient desynchronization. The traces in the middle panel give the mean voltages for the system, and the horizontal line gives the control activation threshold. We see in the third panel that desynchronization occurs, but requires more applications of the stimulus than the optimal stimulus, which is expected due to a smaller Lyapunov exponent.*

5.2. Optimally decreasing the peak of a distribution for the thalamus model. We now turn our attention to controlling populations of neurons using the methods described in section 4 to optimally decrease the peak of their phase distribution. Here, we attempt to provide reasonable values for the still undetermined parameters in the Euler–Lagrange equations (21)–(25). Because we have undetermined parameters, we cannot claim to have found an optimal stimulus to minimize our cost function, but we can still gather powerful insight about stimuli that will affect network desynchronization. In order to make explicit comparisons with the optimal stimulus which maximizes the Lyapunov exponent, we take $t_1 = 7.35$ms and $\beta = 40$. We take our initially synchronized distribution to be a normal distribution with standard deviation $\sigma_d = 0.2$ centered at $\theta = 0$, which corresponds to a spiking event. These conditions were chosen as a reasonable approximation of the observed distribution for simulations of network (26) just before the control threshold $\bar{V} = -40$mV is reached. This gives $\theta_M(0) = 0$ and $\rho_M(0) = 1.995$ as initial conditions to (22) and (23); however, we still need to determine $\lambda_1(0)$ and $\lambda_2(0)$. In order to find the best choice of the remaining initial conditions, we minimize the cost function for reasonable choices of $\lambda_1(0)$ and $\lambda_2(0)$. Using this approach, we find that $\lambda_1(0) = 18$ and $\lambda_2(0) = 2$ approximately minimizes the cost function and gives the stimulus shown in Figure 12, which will be referred to as u_D.

We apply u_D to (15) and (26) with $N = 250$, $D = 0$, and $\alpha_{ij} = 0$ to determine the validity of the results found using the phase reduction. Throughout the simulation, we infer the phase of each neuron in (26) by simulating each neuron separately in the absence of DBS input and

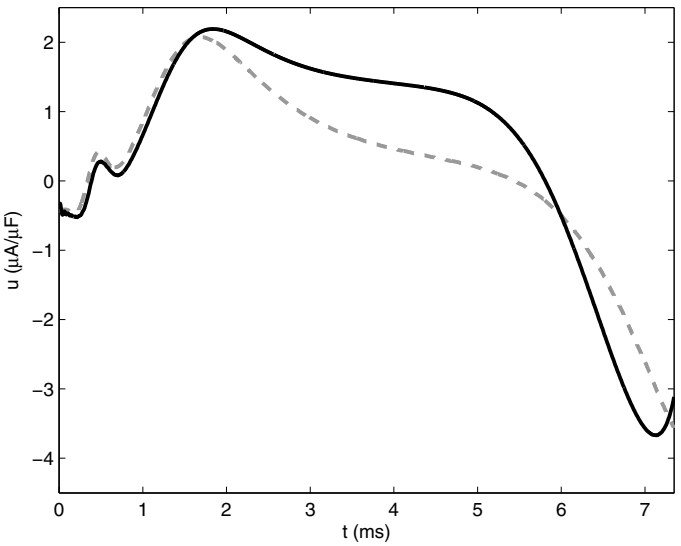

Figure 12. *The optimal stimulus u_D for decreasing the peak of the phase distribution is shown as a solid black line. For reference, the NCB optimal stimulus for maximizing the Lyapunov exponent is shown as a grey dashed line.*

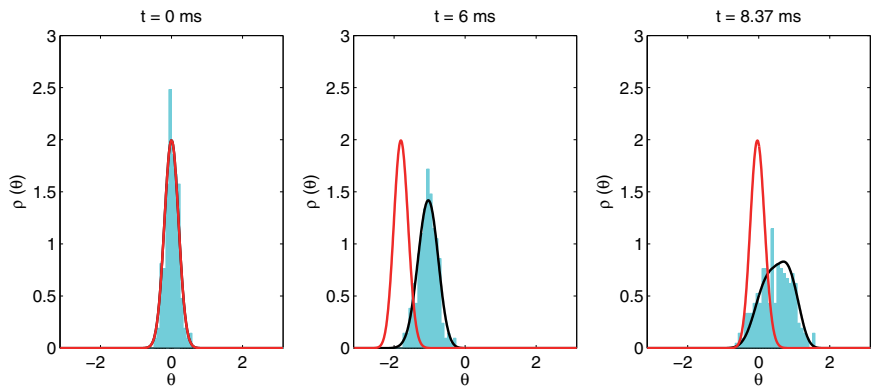

Figure 13. *Three panels from the accompanying animation* (90170_01.avi [local/web 5.49MB]). *In order to clearly present the results, the mapping $\theta \in (\pi, 2\pi) \to (-\pi, 0)$ is used; e.g., $\theta = \frac{3\pi}{2}$ is plotted as $\theta = -\frac{\pi}{2}$. Theoretical and numerical evolutions are shown in black and blue, respectively. The red curve gives the theoretical evolution of the distribution in the absence of stimulus and is shown for reference.*

noise to determine when its next spiking event occurs. The phase evolution is illustrated in the accompanying animation (90170_01.avi [local/web 5.49MB]). Figure 13 shows three frames from this animation. In order to clearly present the results, the mapping $\theta \in (\pi, 2\pi) \to (-\pi, 0)$ is used; e.g., $\theta = \frac{3\pi}{2}$ is plotted as $\theta = -\frac{\pi}{2}$. Theoretical and numerical evolutions are shown in black and blue, respectively. The red curve gives the theoretical evolution of the distribution in the absence of stimulus and is shown for reference. Throughout the simulation, the dynamics of the 250 neuron system are well approximated by (15), and the optimal stimulus brings

ρ_M from 1.995 to 0.776. We now see the utility of the approach which minimizes the peak of the distribution compared to an approach which maximizes the NCB Lyapunov exponent (producing a stimulus we will refer to as u_Λ). From (22), we see that a stimulus has the potential to greatly decrease a distribution when $|Z'(\theta_M)|$ is relatively large. For the thalamus model, this can be done by applying a large negative stimulus when $\theta_M \approx 5.8$. As shown in Figure 12, u_D and u_Λ are nearly identical for $0 \leq t < 2$, but from about $2 \leq t < 6$, $u_D > u_\Lambda$ at a time when $Z(\theta_M) > 0$ and $Z'(\theta_M) \approx 0$. This has the effect of speeding up the distribution but not decreasing the peak height, as demonstrated in 90170_01.avi [local/web 5.49MB]. The extra effort used in speeding up the peak is repaid when $\theta_M \approx 5.8$, when a large negative stimulus decreases the peak rapidly at a time when $Z'(\theta) < 0$. The distribution deforms in such a way that ρ_M remains at $\theta_M \approx 5.8$ longer than we would expect for a system of only two neurons, which is reflected in the inequality $u_D < u_\Lambda$ for $t \approx 6$.

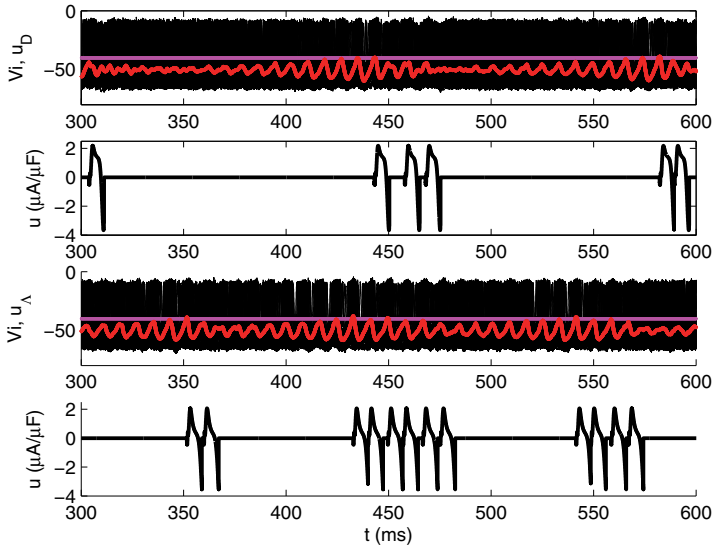

Figure 14. *Comparing u_D to u_Λ. Representative excerpts from a 1000ms simulation using u_D (top) or u_Λ (bottom) as the control.*

We have found stimuli for desynchronizing neural networks using two different approaches. Both approaches produce similar results, but we would like to know if one is better than the other. To answer this question, we simulate (26) with $N = 250$, $D = 1$, and $\alpha_{ij} = 0.1$ for 1000ms using the same control strategy as for the simulations from Figure 10. The initial phase distribution is drawn from a normal distribution with $\sigma_d = 0.2$ centered at $\theta = 0$. A representative portion of the comparison is shown in Figure 14. When we use u_D as the control, the overall energy use is 533 units, while for u_Λ the energy consumption is 460 units. In terms of energy, u_D performs slightly worse than u_Λ, most likely because the neuron distribution is not quite Gaussian throughout the simulation as we had assumed to derive u_D, but both strategies yield an effective control input using a comparable amount of energy. We also note that u_D desynchronizes the network more quickly than u_Λ as calculated from (4). This is

expected because the Lyapunov exponents for u_D and u_Λ as calculated from (4) are 0.107 and 0.066, respectively. However, u_D requires more energy per application of the stimulus.

5.3. Maximizing Lyapunov exponents for the reduced Hodgkin–Huxley model. We next apply our optimization method to a population of neurons, each described by a two-dimensional reduction of the renowned four-dimensional Hodgkin–Huxley (HH) model [12] that reproduces the essential characteristics of a neuron's dynamical behavior (cf. [19], [13]). An alternative strategy for desynchronizing populations of such neurons was investigated in [24]; we will make comparisons with that method later in the present paper. The population of neurons is modeled as follows:

$$\begin{aligned} \dot{V}_i &= f_V(V_i, n_i) + \frac{1}{N}\sum_{i=1}^{n} \alpha_{ij}(V_j - V_i) + u(t) + \eta_i(t), \\ \dot{n}_i &= f_n(V_i, n_i). \end{aligned} \tag{28}$$

Here, $i = 1, \ldots, N$, where N is the total number of neurons; V_i and n_i are membrane voltage and gating variables for neuron i; α_{ij} characterizes the coupling strength between electrotonically coupled neurons i and j [18], with $\alpha_{ij} = \alpha_{ji}$ and $\alpha_{ii} = 0$ for all i; $\eta_i(t) \in \sqrt{2D}\mathcal{N}(0,1)$ is the noise associated with each neuron, assumed to be zero-mean Gaussian white noise with variance $2D$; and $u(t) = I(t)/C$ represents a common control input, where $I(t)$ is a DBS input current in $\mu A/\mu F$ and $C = 1\mu F/cm^2$ is the membrane capacitance. Furthermore,

$$\begin{aligned} f_V &= (I_b - \bar{g}_{Na}[m_\infty(V)]^3(0.8 - n)(V - V_{Na}) - \bar{g}_K n^4(V - V_k) - \bar{g}_L(V - V_L))/C, \\ f_n &= a_n(v)(1 - n) - b_n(V)n. \end{aligned}$$

Other functions and parameters for the reduced model are

$$\begin{aligned} m(V) &= \frac{a_m(V)}{a_m(V) + b_m(V)}, \\ a_m(V) &= 0.1(V + 40)/(1 - \exp(-(V + 40)/10)), \\ b_m(V) &= 4\exp(-(V + 65)/18), \\ a_n(V) &= 0.01(V + 55)/(1 - \exp(-(V + 55)/10)), \\ b_n(V) &= 0.125\exp(-(V + 65)/80, \end{aligned}$$

$$\begin{aligned} V_{Na} &= 50\text{mV}, \quad V_K = -77\text{mV}, \quad V_L = -54.4\text{mV}, \\ \bar{g}_{Na} &= 120\text{mS/cm}^2, \quad \bar{g}_K = 36\text{mS/cm}^2, \\ \bar{g}_L &= 0.3\text{mS/cm}^2, \quad c = 1\mu\text{F/cm}^2, \\ I_b &= 10\mu\text{A/cm}^2. \end{aligned}$$

Here, $\bar{g}_{Na}$, $\bar{g}_K$, and $\bar{g}_L$ represent the conductances of the sodium, potassium, and leakage channels, respectively, and V_{Na}, V_K, and V_L are their respective reversal potentials. Note that I_b, the neuron's baseline current, represents the effect of the surrounding brain regions on the neuron. This is a bifurcation parameter, with the value $I_b = 10\mu\text{A/cm}^2$ chosen to

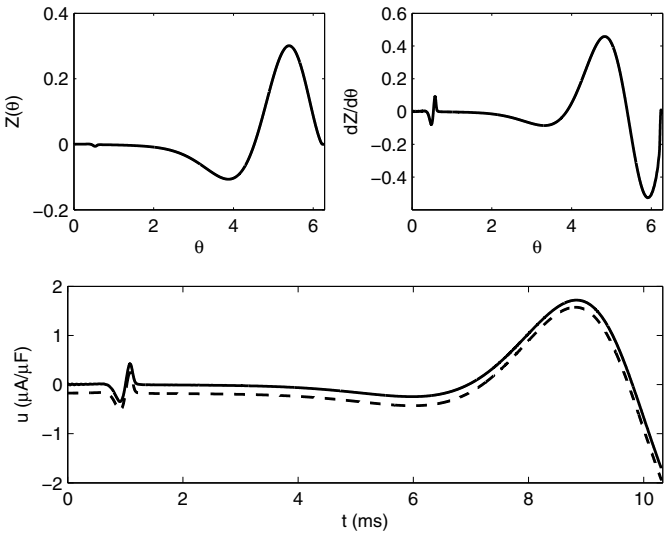

Figure 15. *Top panels show the numerically computed PRC (left) and its derivative (right) for the reduced HH model. The bottom panel shows the CB and NCB optimal stimuli as dashed and solid lines, respectively.*

ensure that the neuron is in an oscillatory (periodically spiking) regime. The natural period, T, of oscillation is 11.81ms.

The PRC, $Z(\theta)$, for this system is computed numerically with the software XPP [6] and is shown in Figure 15. To perform computations with the PRC, we approximate it as a Fourier series with 1200 terms. We take this many terms to get a reasonably nonoscillatory estimate of $Z'''(\theta)$ when solving (24).

The bottom panel of Figure 15 shows the result of the optimization process with and without the CB constraint for the choice of parameters $t_1 = 10.34$ms (corresponding to $\theta = 5.5$ on the limit cycle) and $\beta = 9$. Note that t_1 sets the duration of the stimulus and could be chosen differently, provided that it is sufficiently smaller than the natural period, T, of the neuron, and β is chosen so that a positive Lyapunov exponent is favored but also such that the magnitude of the control input will be small enough so that the phase reduction is still valid. We find that the CB stimulus looks nearly identical to the NCB stimulus except for a downward shift. This is to be expected since, as is the case in the thalamus model, the NCB stimulus is nearly CB. Also, we find that the optimal control looks similar to the derivative of the PRC, as shown in Figure 15. An explanation for this phenomenon is given in section 5.1.

Panels (A) and (B) in Figure 16 show the phase difference between two neurons with nearly identical initial phases, subject to the NCB optimal stimulus shown in Figure 15. The optimal stimulus is event-based and is applied every time the phase of the trailing neuron crosses $\theta = 0$. Panels (C) and (D) show the results of a similar test with the CB stimulus. The Lyapunov exponents, Λ, for the NCB and CB stimuli are found to be 0.0823 and 0.0782, respectively. Dashed lines show exponential functions based on the Lyapunov exponents. We find that all of the plots match closely until $\phi \approx 1$, with the NCB stimulus performing slightly better than the CB stimulus. In this case, balancing charge comes at the cost of degrading

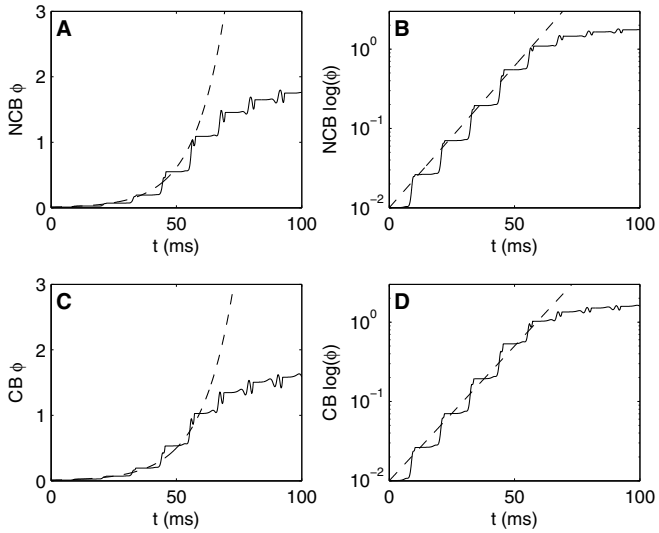

Figure 16. (A)–(B) *The phase difference between two neurons over time for the NCB optimal stimulus (giving* $\Lambda = 0.0823$*) applied repeatedly to two neurons with nearly identical initial phases.* (C)–(D) *The same plots for the CB stimulus* ($\Lambda = 0.0782$)*. In both cases the neurons desynchronize at a rate determined by* Λ*, calculated from* (4)*, until* $\phi \approx 1$*. Dashed lines show exponential functions based on the Lyapunov exponents.*

performance.

It is natural to wonder to what degree the optimal control found from the phase model will desynchronize neurons that obey the set of equations with which we started. To this end, we simulate the deterministic version of equations (28), i.e., with $D = 0$, using a fourth order Runge–Kutta solver. The top panel in Figure 17 shows the time histories of three neurons with initial conditions that correspond to $\theta = -0.1,\ 0,$ and $+0.1$ on the periodic orbit. The control is applied every time the reference neuron, with initial phase $\theta = 0$, fires. Figure 17 also shows the input for reference. We find that after 90ms, the neuron that started at $\theta = +0.1$ now fires approximately 6ms after the reference neuron, while the neuron that started at $\theta = -0.1$ fires approximately 2 milliseconds before the reference neuron. The reason for this discrepancy can be explained by noting the shape of the PRC. We see in Figure 15 that the PRC has a local minimum at $\theta \approx 4$. Approximately 9ms after the optimal stimulus is first presented, the remaining stimulus has negative sign, the reference neuron has a phase corresponding to a positive value on the PRC, and the neuron which starts behind has a phase of $\theta \approx 4$. Because of these conditions near the end of the cycle, the optimal stimulus brings the phases closer together, negating the desynchronization achieved earlier in the cycle.

We now apply this optimal control to a network of $N = 100$ coupled, initially synchronized, noisy neurons, with an identical coupling strength of $\alpha_{ij} = 0.05$ and i.i.d. noise with $D = 0.7$. The control logic used is similar to the logic presented in section 5.1, with the controller switching to the *inactive* state if spikes remain below -40mV and switching back to the *active* state if a spike registers above -30mV.

Figure 18 shows the result of this simulation. The top panel shows voltages of each neuron

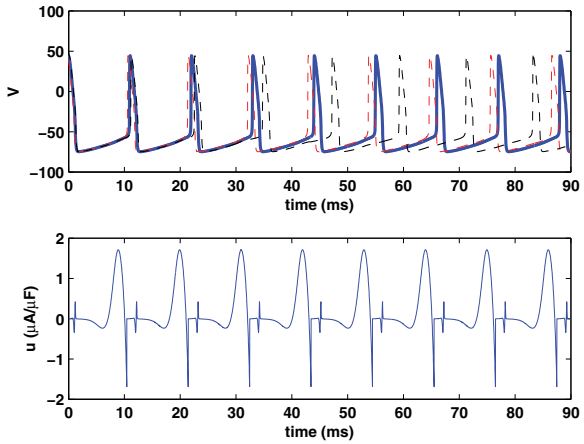

Figure 17. *Top: Time histories of three neurons with initial conditions* $\theta = -0.1,\ 0, \text{and } +0.1$ *on the periodic orbit. A new stimulus is applied each time the reference neuron with initial phase* $\theta = 0$ *(shown as a black line) fires. Once the neurons are no longer close in phase, the neuron which started ahead of the reference neuron desynchronizes faster than the neuron that starts behind the reference neuron, which can be explained by the shape of the PRC, as described in the main text. Bottom: Input to the neurons modeled above.*

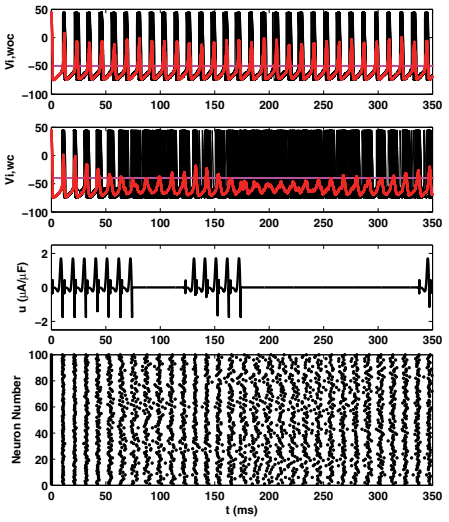

Figure 18. *Results for a population of* $N = 100$ *noisy, coupled neurons obeying the reduced HH model. The top panel shows results in the absence of control. The second and third panels show results for the same network with the event-based control applied. The traces give the mean voltages for the system, and the horizontal line shows the control activation threshold. Substantial desynchronization can be seen from the raster plot.*

as well as the average voltage of the coupled noisy system without control. We find that $\bar{V}$ peaks near 0mV throughout the simulation, and the neurons stay synchronized. The second panel shows the individual neuron voltages and mean voltage for the same coupled system with both noise and control input. The horizontal line in this panel represents the threshold

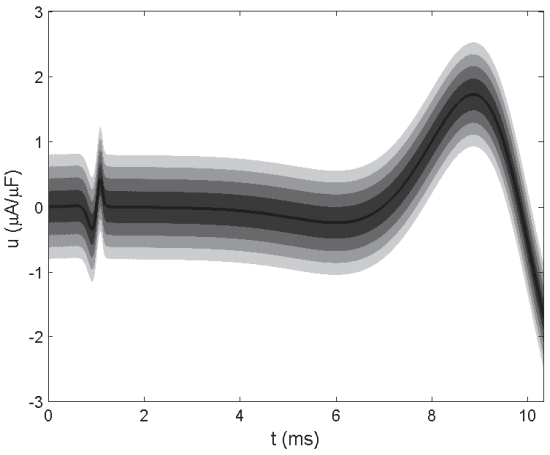

Figure 19. *The optimal NCB stimulus, shown as a solid line, yields* $\Lambda = 0.0823$. *In order to guarantee a stimulus with* $\Lambda \geq 0.06$, 0.04, 0.02, *and* 0, *we require* $||I_e(t)|| \leq 0.242$, 0.440, 0.615, *and* 0.797, *respectively, for all* t. *Darker shaded regions on the plot correspond to regions with larger guaranteed Lyapunov exponents.*

voltage of −30mV. The control input is shown in the third panel. Clearly the control input desynchronizes the network of neurons, as seen from the raster plot, and since the control is event-based, it needs to be turned on only once $\bar{V}$ crosses the threshold line.

In an experimental setting, it is unlikely that the optimal desynchronizing stimulus $I_{opt}(t)$ can be found exactly. For this reason, we would like to calculate bounds on $I_e(t)$, where $I(t) = I_{opt}(t) + I_e(t)$ with $I(t)$ found using an experimentally obtained PRC such that we can guarantee a given Lyapunov exponent. Using the strategy developed in section 3, we can determine a worst case Λ for a particular $||I_e||_\infty$. Here, we use a shooting method to determine that, in order to guarantee stimuli with $\Lambda \geq 0.06$, 0.04, 0.02, and 0, we require $||I_e(t)|| \leq 0.242$, 0.44, 0.615, and 0.797, respectively, for all t. Graphical representations of these error bounds are shown in Figure 19. We emphasize that these are only bounds that will *guarantee* a certain value of Λ. As in section 5.1, even if a stimulus falls outside of a shaded region, the associated Λ may still be larger than the value guaranteed for that shaded region. For a network of neurons without coupling or noise, any stimulus with $\Lambda > 0$ should be able to desynchronize an initially coupled neural network. However, for real networks, the value of Λ required for desynchronization will depend on the strength of the coupling and noise.

We now compare the energy used by our NCB, event-based control shown in Figure 15 (which we will refer to as the exponential control) to the energy used by a control that will desynchronize a system of neurons by optimally driving them to a phaseless set as developed by Nabi et al. in [24] (which we will refer to as the phaseless control). For a system obeying Ohm's law, the power P applied by an input is given by $P \sim u^2$. A representative portion of a comparison over 1500ms is shown in Figure 20. The top two panels show a noisy system of coupled neurons stimulated by the exponential control, while the bottom two panels show the same system stimulated by the phaseless control.

For a single application of the exponential control, $\int_0^{t_1} u^2(t) \approx 2.32$, while for one application of the phaseless control, $\int_0^{T_{end}} u^2(t) \approx 194$. Throughout the simulation, the exponential

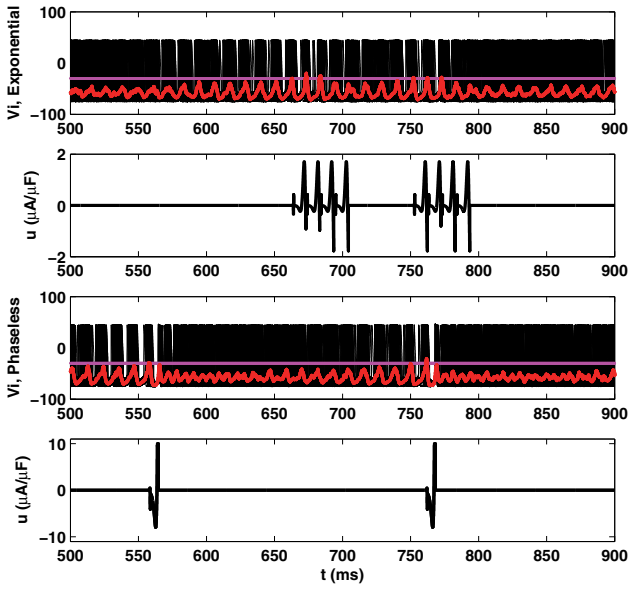

Figure 20. *Comparing the NCB optimal (exponential) control to the control presented in* [24] *(phaseless). Representative excerpts from a* 1500*ms test of the exponential and phaseless control are shown in the top two and bottom two panels, respectively. The exponential control fires more often than the phaseless control (compare second and fourth panels) but uses less energy because the magnitude of the stimulus is much smaller.*

control is active for more time than the phaseless control; however, one cycle of the exponential control costs much less than one cycle of the phaseless control. Over the entire 1500ms simulation, we find that the total power used is proportional to 236 and 1904 for the exponential and phaseless controls, respectively. Not only is the maximum applied control much less for the exponential control, but it also uses nearly an order of magnitude less energy.

5.4. Optimally decreasing distribution peak height for the reduced HH model. Finally, we look from the perspective of controlling distributions by using the strategy described in section 4 to see if we can find a more effective control to desynchronize (28) than the control that maximizes the Lyapunov exponent. Here, we attempt to provide reasonable values for the still undetermined parameters in the Euler–Lagrange equations (21)–(25). Because we have undetermined parameters, we cannot claim to have found an optimal stimulus to minimize our cost function, but we can still gather powerful insight about stimuli that will affect network desynchronization. In order to make explicit comparisons to the optimal stimulus which maximizes the Lyapunov exponent, we take $t_1 = 10.34$ms. We choose $\beta = 8$ this time because $\beta = 9$ gives a solution which is too large in magnitude and invalidates the phase reduction. As in section 5.2, we take our initially synchronized distribution to be a normal distribution with standard deviation $\sigma_d = 0.2$ centered at $\theta = 0$. These conditions were chosen as a reasonable approximation to observed distributions for simulations of the network (28) just before the control threshold $\bar{V} = -30$mV is reached. This gives $\theta_M(0) = 0$ and $\rho_M = 1.995$ as initial conditions for (22) and (23). We optimize the cost function over reasonable values of $\lambda_1(0)$,

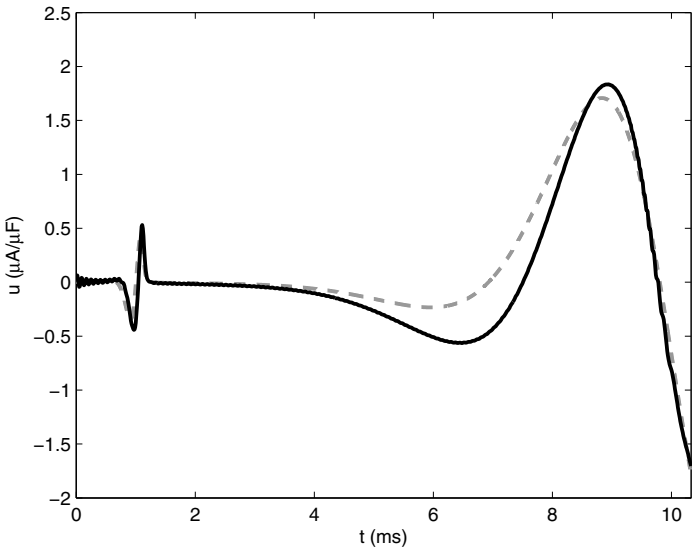

Figure 21. *The optimal stimulus for decreasing the peak of a distribution is shown as a solid black line. For reference, the NCB optimal stimulus for maximizing the Lyapunov exponent is shown as a grey dashed line.*

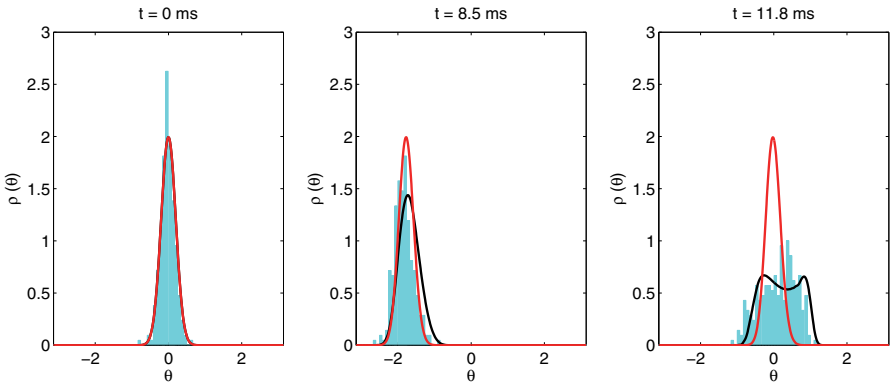

Figure 22. *Three frames from the accompanying animation* (90170_02.avi [local/web 4.40MB]). *In order to clearly present the results, the mapping* $\theta \in (\pi, 2\pi) \to (-\pi, 0)$ *is used; e.g.,* $\theta = \frac{3\pi}{2}$ *is plotted as* $\theta = -\frac{\pi}{2}$. *Theoretical and numerical evolutions are shown in black and blue, respectively. The red curve gives the theoretical evolution of the distribution in the absence of stimulus and is shown for reference.*

$\lambda_2(0)$ in order to find the best choice for the remaining initial conditions. Using this approach, we find that $\lambda_1(0) = 6$ and $\lambda_2(0) = 0$ approximately minimizes the cost function and gives the stimulus shown in Figure 21, which will be referred to as u_D.

We apply u_D to (15) and (28) with $N = 250$, $D = 0$, and $\alpha_{ij} = 0$ to determine the validity of the results found using the phase reduction. For a given neuron, we can deduce its phase at a given time by integrating the reduced HH equations without input or noise until the neuron's next spike. The phase evolution is shown in the accompanying file (90170_02.avi [local/web 4.40MB]); Figure 22 shows three frames from this animation. In order to clearly

present the results, the mapping $\theta \in (\pi, 2\pi) \to (-\pi, 0)$ is used; e.g., $\theta = \frac{3\pi}{2}$ is plotted as $\theta = -\frac{\pi}{2}$. Theoretical and experimental evolutions are shown in black and blue, respectively. The red curve gives the theoretical evolution of the distribution in the absence of stimulus and noise and is shown for reference. Throughout the simulation, the phase reduction well approximates the dynamics of the 250 neuron system, and the optimal stimulus takes ρ_M from 1.995 to approximately 0.7. The stimuli u_D and u_Λ are nearly identical for the reduced HH mode, with discrepancies in the two answers most likely due to the more restrictive constraints on u_Λ. The similar answers are of interest because we approached the desynchronization problem from two different perspectives.

To gauge whether u_D is an improvement over u_Λ, we simulate (28) using the same parameters and control strategy as for the simulations from Figure 18. When we use u_D as the control, the overall energy use is 270 units, while for I_Λ the energy consumption is 214 units. This discrepancy is most likely because the assumption that u_D is Gaussian is no longer valid near the end of the cycle, which wastes a small amount of energy. Results for this simulation do not differ significantly from the results in Figure 18 and are not shown.

5.5. Comparison to pulsatile input. As mentioned in section 1, clinical DBS is currently implemented with a high-frequency pulsatile input. While the exact mechanism by which this wave form mitigates the symptoms of Parkinson's disease is unknown, Wilson, Beverlin, and Netoff [41] postulated that DBS may be effective because it chaotically desynchronizes neurons in the thalamus region of the brain. They used phase reduction to show that, for certain stimulus intensities with frequencies that are approximately twice the natural frequency ($2\times\frac{1}{T}$) of a neuron, pulsatile stimuli can effectively desynchronize a population of neurons. Using the same conventions as [41], we take $\theta \in [0, 1)$ with $\theta = 0$ corresponding to the spiking of a neuron and scaled to 1 time unit. We use the same PRC as in [41], and apply our NCB and CB optimization process with $\beta = 1.5$ and $t_1 = 0.85$. The PRC, its first derivative, and the resulting optimal stimuli are shown in Figure 23.

The respective Lyapunov exponents for the NCB and CB optimal stimuli from (4) are 1.429 and 1.937, with respective power consumptions ($\int_0^{t_1} u^2 dt$) of 1.11 and 1.99. We note that the CB stimulus outperforms the NCB stimulus at the expense of using almost twice as much energy. Figure 24 shows the phase separation of two neurons which obey (2) for the PRC shown in Figure 23, subject to repeated iterations of both the NCB (panels (A) and (B)) and CB (panels (C) and (D)) stimuli. As seen in previous sections, the neurons exponentially desynchronize at a rate determined by their Lyapunov exponents until the neurons are nearly antiphase.

We now apply the NCB optimal stimulus to a population of 100 noisy neurons:

$$\dot{\theta}_i = \omega + Z(\theta_i)\left[u(t) + A\gamma_i(t) + B\zeta(t)\right] + \frac{A^2 + B^2}{2} Z(\theta_i)Z'(\theta_i), \quad i = 1, \ldots, 100, \tag{29}$$

where $\omega = 1$ gives the neural baseline dynamics (recall that $\theta \in [0, 1)$), γ and ζ are individual and common white noise processes with strength $A = \sqrt{0.2}$ and $B = \sqrt{0.3}$, respectively, and $u(t)$ is the common DBS input. The final term in (29) corresponds to the Ito term for the phase reduction [8]. In order to determine when the optimal stimulus should be presented, we need to know when the average phase of the system of neurons is $\theta = 0$. In real neurons, a

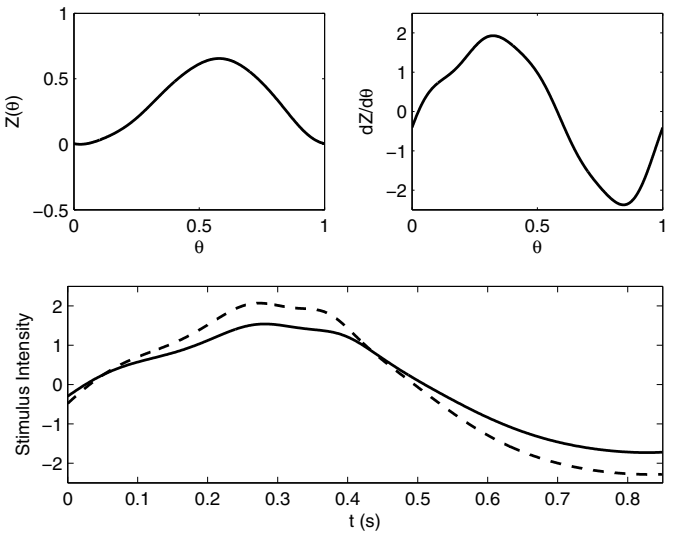

Figure 23. *Top panels show the PRC and its derivative for the model used in* [41]. *The bottom panel shows the CB and NCB optimal stimuli as dashed and solid lines, respectively.*

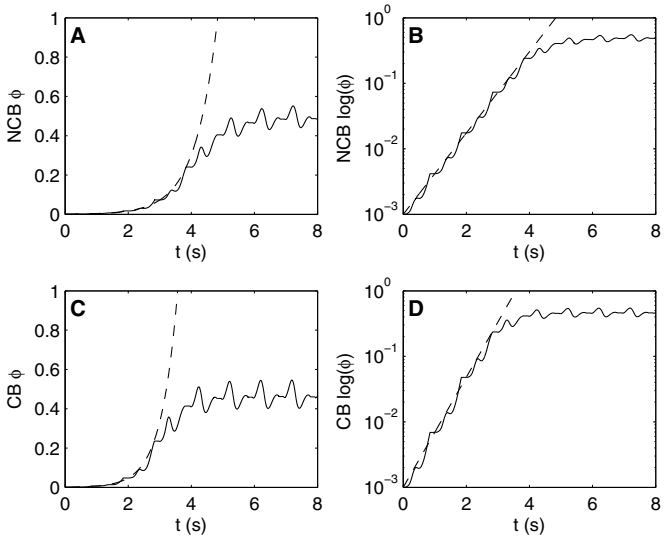

Figure 24. (A)–(B) *The phase difference between two neurons over time for the NCB optimal stimulus (giving* $\Lambda = 1.429$*) applied repeatedly to two neurons with nearly identical initial phases.* (C)–(D) *The same plots for the CB stimulus (*$\Lambda = 1.937$*). In both cases the neurons desynchronize at a rate determined by* Λ*, calculated from* (4) *until* $\phi \approx 0.25$*, at which point the solution begins to asymptotically approach* $\phi \approx 0.5$*, i.e., the antiphase state. Dashed lines show exponential functions based on the Lyapunov exponents.*

spiking event is defined to be $\theta = 0$ and can be observed as a sudden increase in voltage. For the model under consideration, we are simulating a phase reduced model, with no observable

voltage spikes. In lieu of $\bar{V}$ for the system of neurons, we monitor the average phase of the system, $\bar{\theta} = \frac{1}{N}\sum_{i=1}^{N}\theta_i$. Note that $\bar{\theta}$ is equivalent to ψ in the first order Kuramoto parameter, $re^{i\psi} = \frac{1}{N}\sum_{j=1}^{N} e^{i\theta_j}$. For a completely synchronized network, $\bar{\theta}$ varies between 0 and 1, while for a network in the splay state, $\bar{\theta}$ remains constant at 0.5. This gives a continuum from which we can qualitatively gauge the level of synchronization by noting the maximum value of $\bar{\theta}$ on a particular cycle. To determine when to apply a new stimulus, a flag is set when $\bar{\theta} > 0.65$, indicating that the network is still sufficiently synchronized, and a new stimulus begins if the flag is set and $\bar{\theta} < 0.5$, indicating that a majority of the neurons have phase $\theta \approx 0$.

To characterize the desynchronization of the neural network, following [41], we use the entropy

$$\text{Entropy} = \sum_{\mathrm{j}=1}^{\mathrm{B}} \mathrm{p}(\psi_{\mathrm{j}}) \log(\mathrm{p}(\psi_{\mathrm{j}})),$$

where $p(\psi_j)$ is the probability of being in bin j of B total bins. The splay state has the highest entropy for a population of 100 neurons at 4.6.

We note that the results from [41] were computed using a mapping based on the PRC to determine the effect of a DBS pulse. In our trials, we found that adding pulse width somewhat degraded the effectiveness of the pulsatile stimulus. In order to replicate Wilson's results and make comparisons, we use (29) with $u(t) = 0$ for all time, and instead iterate when a pulse stimulus is presented as follows:

$$\theta_{i+1} = \theta_i + Z(\theta_i)\delta,$$

where δ is the amplitude of the stimulus. For the simulation, we choose $\delta = 0.63$ at a frequency of 1.92Hz. These values are in the range with the best desynchronization capabilities for this model [41]. We use an Euler–Maruyama method [11] to solve (29) for both the optimal and pulsatile stimulus, with results shown in Figure 25. We find that both stimuli are able to desynchronize the population to similar levels as characterized by the entropy of the system. However, the pulsatile input takes approximately 15 seconds and 29 pulses for the entropy to reach a reasonably steady entropy value of 3.5, while it only takes 5 seconds and three applications of the optimal stimulus to increase the entropy to 3.5. Assuming the power usage $P \sim u^2$, we cannot directly approximate the energy required by the pulsatile input since it has no pulse-width (PW). However, in human trials, [5] and [39] used pulsatile inputs with a PW-to-period ratio of 7.8×10^{-3} and 9.5×10^{-3}, respectively. We take the average of these two ratios to estimate a PW and require $\mathrm{PW} \cdot \mathrm{u} = \delta$, and we find that PW ~ 0.0045 and $u \sim 155$ in order to be therapeutically effective. Letting the power consumption $P = u^2 \cdot \mathrm{PW}$, we find that $P \sim 108$ units. Conversely, for the optimal stimulus, $\int_0^{t_1} u^2 dt \sim 1.11$. As a very rough estimate of total energy used to achieve steady desynchronization, three applications of the optimal stimulus use 3.33 units of energy, while 29 applications of the pulsatile stimulus use 3132 units of energy. Both stimuli are able to desynchronize the neural network, but the optimal stimulus is able to do so using three orders of magnitude less energy.

6. Conclusion. We have described two methods for desynchronizing neural networks: by optimally maximizing the Lyapunov exponent (4) and by optimally decreasing the peak height of the phase distribution. Most notably, while each of these methods is based on a different perspective, they produce answers that are quite similar. We find that the method

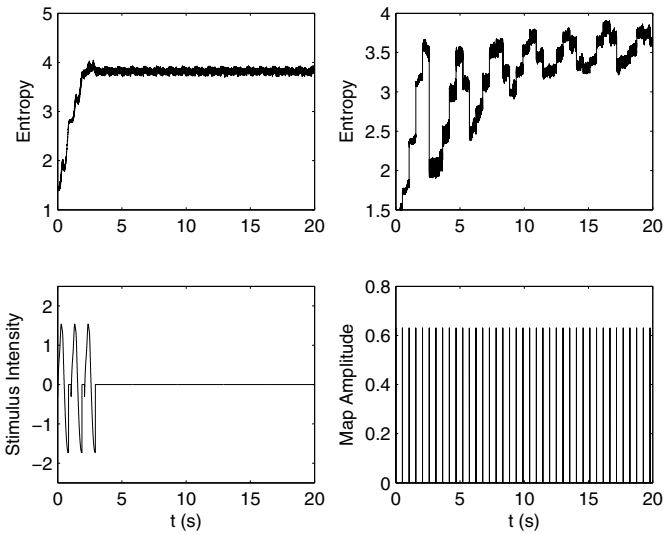

Figure 25. *Left panels show the entropy of* 100 *neurons (top) and the applied stimulus for the exponentially desynchronizing control (bottom). Right panels show entropy of* 100 *neurons for the pulsatile input applied at* 1.92 *Hz. Note that the bottom-right panel shows the map amplitude, δ, and not the stimulus intensity to emphasize that the stimuli are simulated as delta functions. Each pulse uses* 108 *units of energy.*

for optimally maximizing the Lyapunov exponent uses three orders of magnitude less energy than a method that uses pulsatile stimuli to achieve desynchronization, which represents an enormous potential savings in battery life of a pacemaker and could also mitigate some of the negative side-effects of DBS. We have also shown that the approach of maximizing the Lyapunov exponent is robust to inaccuracies in finding the optimal stimulus and found bounds for a stimulus derived from a network without coupling that will guarantee a minimum Lyapunov exponent required to give desynchronization for a given network with coupling. Because this method is robust to inaccuracies, it has potential to work well in an in vitro setting and could realistically provide an effective treatment for Parkinson's disease.

REFERENCES

[1] A. Abouzeid and B. Ermentrout, *Type-*II *phase resetting curve is optimal for stochastic synchrony*, Phys. Rev. E, 80 (2009), 011911.

[2] E. Brown, J. Moehlis, and P. Holmes, *On the phase reduction and response dynamics of neural oscillator populations*, Neural Comput., 16 (2004), pp. 673–715.

[3] P. Danzl, J. Hespanha, and J. Moehlis, *Event-based minimum-time control of oscillatory neuron models*, Biol. Cybernet., 101 (2009), pp. 387–399.

[4] P. Danzl, A. Nabi, and J. Moehlis, *Charge-balanced spike timing control for phase models of spiking neurons*, Discrete Contin. Dyn. Syst., 28 (2010), pp. 1413–1435.

[5] G. Deuschl, C. Schade-Brittinger, P. Krack, J. Volkmann, H. Schafer, K. Botzel, C. Daniels, A. Deutschlander, U. Dillmann, W. Eisner, D. Gruber, W. Hamel, J. Herzog, R. Hillker, S. Klebe, M. Klob, J. Kay, M. Krause, A. Kupsch, D. Lorenz, S. Lorenzl, M. Mehdorn, J. R. Moringlane, W. Oertel, M. Pinsker, H. Reichmann, A. Reub, G. H. Schneider, A. Schnitzler, U. Steude, V. Sturm, L. Timmermann, V. Tronnier, T. Trottenberg,

L. Wojtecki, E. Wolf, W. Poewe, and J. Voges, *A randomized trial of deep-brain stimulation for Parkinson's disease*, N. Engl. J. Med., 355 (2006), pp. 896–908.
[6] B. Ermentrout, *Simulating, Analyzing and Animating Dynamical Systems: A Guide to XPPAUT for Researchers and Students*, Software Environ. Tools 14, SIAM, Philadelphia, 2002.
[7] D. B. Forger and D. Paydarfar, *Starting, stopping, and resetting biological oscillators: In search of optimal perturbations*, J. Theoret. Biol., 230 (2004), pp. 521–532.
[8] C. W. Gardiner, *Handbook of Stochastic Methods: For Physics, Chemistry and the Natural Sciences*, Springer, Berlin, 2004.
[9] C. Hammond, H. Bergman, and P. Brown, *Pathological synchronization in Parkinson's disease: Networks, models and treatments*, Trends Neurosci., 30 (2007), pp. 357–364.
[10] C. Hauptmann, O. Popovych, and P. Tass, *Effectively desynchronizing deep brain stimulation based on a coordinated delayed feedback stimulation via several sites: A computational study*, Biol. Cybern., 93 (2005), pp. 463–470.
[11] D. J. Higham, *An algorithmic introduction to numerical simulation of stochastic differential equations*, SIAM Rev., 43 (2001), pp. 525–546.
[12] A. L. Hodgkin and A. F. Huxley, *A quantitative description of membrane current and its application to conduction and excitation in nerve*, J. Physiol., 117 (1952), pp. 500–544.
[13] A. L. Hodgkin and A. F. Huxley, *Canards for a reduction of the Hodgkin-Huxley equations*, J. Math. Biol., 52 (2006), pp. 141–53.
[14] R. Honeycutt, *Stochastic Runge-Kutta algorithms.* I. *White noise*, Phys. Rev. A, 45 (1992), pp. 600–603.
[15] L. Iasemidis, D. Shiau, J. Sackellares, P. Pardalos, and A. Prasad, *Dynamical resetting of the human brain at epileptic seizures: Application of nonlinear dynamics and global optimization techniques*, IEEE Trans. Biomed. Eng., 51 (2004), pp. 493–506.
[16] L. Iasemidis, D. Shiau, W. W. Chaovalitwongse, J. Sackellares, P. Pardalos, J. Principe, P. Carney, A. Prasad, B. Veeramani, and K. Tsakalis, *Adaptive epileptic seizure prediction system*, IEEE Trans. Biomed. Eng., 50 (2003), pp. 616–627.
[17] E. M. Izhikevich, *Dynamical Systems in Neuroscience: The Geometry of Excitability and Bursting*, MIT Press, London, 2007.
[18] D. Johnston and S. M.-S. Wu, *Foundations of Cellular Neurophysiology*, MIT Press, Cambridge, MA, 1995.
[19] J. Keener and J. Sneyd, *Mathematical Physiology*, Springer, New York, 1998.
[20] D. Kirk, *Optimal Control Theory*, Dover, New York, 1998.
[21] I. Z. Kiss, C. G. Rusin, H. Kori, and J. L. Hudson, *Engineering complex dynamical structures: Sequential patterns and desynchronization*, Science, 316 (2007), pp. 1886–1889.
[22] M. Luo, Y. Wu, and J. Peng, *Washout filter aided mean field feedback desynchronization in an ensemble of globally coupled neural oscillators*, Biol. Cybern., 101 (2009), pp. 241–246.
[23] D. Merrill, M. Bikson, and J. Jefferys, *Electrical stimulation of excitable tissue: Design of efficacious and safe protocols*, J. Neurosci. Methods, 141 (2005), pp. 171–198.
[24] A. Nabi, M. Mirzadeh, F. Gibou, and J. Moehlis, *Minimum energy desynchronizing control for coupled neurons*, J. Comput. Neurosci., 34 (2013), pp. 259–271.
[25] T. Netoff, M. Schwemmer, and T. Lewis, *Experimentally estimating phase response curves of neurons*, in Phase Response Curves in Neuroscience, N. Schultheiss, A. Prinz, and R. Butera, eds., Springer, New York, 2012, pp. 95–129.
[26] A. Nini, A. Feingold, H. Slovin, and H. Bergman, *Neurons in the global pallidus do not show correlated activity in the normal monkey, but phased locked oscillations appear in the MPTP model of Parkinsonism*, J. Neurophysiol., 74 (1995), pp. 1800–1805.
[27] B. Pakkenberg and H. Gundersen, *Neocortical neuron number in humans: Effect of sex and age*, J. Comp. Neurol., 384 (1997), pp. 312–320.
[28] P. Pardalos and V. Yatsenko, *Optimization approach to the estimation and control of Lyapunov exponents*, J. Optim. Theory Appl., 128 (2006), pp. 29–48.
[29] O. Popovych, C. Hauptmann, and P. Tass, *Effective desynchronization by nonlinear delayed feedback*, Phys. Rev. Lett., 94 (2005), p. 164102.
[30] O. Popovych and P. Tass, *Synchronization control of interacting oscillatory ensembles by mixed nonlinear delayed feedback*, Phys. Rev. E, 82 (2010), 026204.

[31] K. Pyragas, O. Popovych, and P. Tass, *Controlling synchrony in oscillatory networks with a separate stimulation-registration setup*, Europhys. Lett., 80 (2007), 40002.
[32] J. Ritt, *A Probabilistic Analysis of Forced Oscillators with Application to Neuronal Response Reliability*, Ph.D. thesis, Department of Mathematics, Boston University, Boston, 2003.
[33] M. Rosenblum and A. Pikovsky, *Controlling synchronization in an ensemble of globally coupled oscillators*, Phys. Rev. Lett., 92 (2004), 114102.
[34] J. Rubin and D. Terman, *High frequency stimulation of the subthalamic nucleus eliminates pathological thalamic rhythmicity in a computational model*, J. Comput. Neurosci., 16 (2004), pp. 211–235.
[35] S. Schiff, *Neural Control Engineering*, MIT Press, Cambridge, MA, 2011.
[36] S. Talathi, P. Carney, and P. Khargonekar, *Control of neural synchrony using channelrhodopsin-2: A computational study*, J. Comput. Neurosci., 31 (2011), pp. 87–103.
[37] P. Tass, *Desynchronizing double-pulse phase resetting and application to deep brain stimulation*, Biol. Cybern., 85 (2001), pp. 343–354.
[38] P. Tass, *Phase Resetting in Medicine and Biology: Stochastic Modelling and Data Analysis*, Springer, New York, 2007.
[39] S. Thobois, P. Mertens, M. Guenot, M. Hermier, H. Mollion, M. Bouvard, G. Chazot, E. Broussolle, and M. Sindou, *Subthalamic nucleus stimulation in Parkinson's disease clinical evaluation of 18 patients*, J. Neurol., 249 (2002), pp. 529–543.
[40] N. Tukhlina, M. Rosenblum, A. Pikovsky, and J. Kurths, *Feedback suppression of neural synchrony by vanishing stimulation*, Phys. Rev. E, 75 (2007), p. 011918.
[41] C. Wilson, B. Beverlin II, and T. Netoff, *Chaotic desynchronization as the therapeutic mechanism of deep brain stimulation*, Front. Syst. Neurosci., 5 (2011), 50.